

## LIMITS ON *I*-BAND MICROVARIABILITY OF THE GALACTIC BULGE MIRAS

P. R. WOŹNIAK, K. E. MCGOWAN, AND W. T. VESTRAND  
 Los Alamos National Laboratory, MS-D436, Los Alamos, NM 87545  
*Draft version February 2, 2008*

### ABSTRACT

We search for microvariability in a sample of 485 Mira variables with high quality *I*-band light curves from the second generation Optical Gravitational Lensing Experiment (OGLE-II). Rapid variations with amplitudes in the  $\sim$ 0.2–1.1 mag range lasting hours to days were discovered in Hipparcos data by de Laverny et al. (1998). Our search is primarily sensitive to events with time-scales of  $\sim$ 1 day, but retains a few percent efficiency (per object) for detecting unresolved microvariability events as short as 2 hours. We do not detect any candidate events. Assuming that the distribution of the event time profiles is identical to that from the Hipparcos light curves we derive the 95% confidence level upper limit of  $0.038 \text{ yr}^{-1} \text{ star}^{-1}$  for the rate of such events (1 per 26 years per average object of the ensemble). The high event rates of the order of  $\sim 1 \text{ yr}^{-1} \text{ star}^{-1}$  implied by the Hipparcos study in the  $H_P$  band are excluded with high confidence by the OGLE-II data in the *I* band. Our non-detection could still be explained by much redder spectral response of the *I* filter compared to the  $H_P$  band or by population differences between the bulge and the solar neighborhood. In any case, the OGLE-II *I*-band data provide the first limit on the rate of the postulated microvariability events in Mira stars and offer new quantitative constraints on their properties. Similar limits are obtained for other pulse shapes and a range of the assumed time-scales and size-frequency distributions.

*Subject headings:* stars: variables, AGB and post-AGB, activity

### 1. INTRODUCTION

Mira variables are a subclass of Red Variables, also known as Long Period Variables (LPVs). They are low mass AGB giants, mostly with M type spectra (e.g. Gautschy & Saio 1996). Their large amplitude light variations on time scales of  $\sim$ 1 year are thought to arise due to the pulsation instability (e.g. Keeley 1970). There are intriguing reports of rapid light variations in Mira stars on time scales of a few days (Maffei & Tosti 1995) or even hours and minutes (Schaefer 1991) with amplitudes in the range 0.1–1.4 mag. The most systematic study of microvariability in Mira stars is based on Hipparcos data (de Laverny et al. 1998, hereafter dL98). It reports the discovery of 51 events in 39 out of 239 observed Mira stars. The amplitudes of events detected by Hipparcos are between 0.2 and 1.1 mag. To best of our knowledge, so far there are no published estimates for the rate of such events. Other reports of rapid variations in broad band photometry of specific Mira variables include Smak & Wing (1979) or more recently de Laverny et al. (1997) and Teets & Henson (2003). From existing data very little can be inferred about the spectral properties of those rapid variations, but microvariability in several spectral features has been reported (Odell et al. 1970, Kovar et al. 1972). On the other hand, Smith et al. (2002) do not detect any rapid variations in the COBE DIRBE mid-infrared light curves of 38 Miras.

Willson & Struck (2002) explored possible interpretations and favored one involving hot flashes due to interaction of the extended Mira atmosphere with a Jovian planet or a brown dwarf. This process was studied numerically by Struck, Cohenim & Willson (2002, 2004). The scenario can explain the time scale of the observed microvariability and produces energies and luminosities

roughly of the right order of magnitude, but it ignores the fact that dL98 have seen approximately equal numbers of positive and negative flux excursions.

Here we use a large set of high quality *I*-band photometry from the Optical Gravitational Lensing Experiment (OGLE) to constrain the rate of microvariability for Mira stars found in the Galactic Bulge.

### 2. DATA AND SAMPLE SELECTION

#### 2.1. *OGLE-II light curves*

We use the photometric data collected, processed and published by the second generation OGLE experiment (OGLE-II; Udalski, Kubiak, & Szymański 1997). Our analysis is based on photometry from Difference Image Analysis (DIA) of the images collected during observing seasons 1997–1999 (Woźniak et al. 2002, Woźniak 2000). The DIA technique relieves numerous complications associated with crowded fields and enabled routine photometry as accurate as 0.5% for bright unsaturated stars like the brightest AGB variables in the Galactic Bulge. This data set contains *I*-band light curves for approximately  $2 \times 10^5$  candidate variable objects with the average time sampling of once every 1–3 days and typically 250 measurements per object. We defer a detailed discussion of the time sampling to Section 3.1. Observations span the magnitude range between 10.5 and 19.5. The total time baseline of the data set is 3 years with 2 inter-season gaps, each lasting about 4 months.

#### 2.2. *Selecting Mira variables*

The General Catalog of Variable Stars (GCVS; Khlopov 1998) states that Mira variables have *V*-band light amplitudes between 2.5 and 11 mag, well pronounced periodicity and periods ranging from 80 to 1000 days. The amplitudes of Miras show a decreasing trend toward the red and the near-infrared part of the spec-

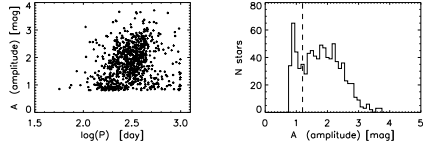


FIG. 1.— Period amplitude distribution (left) and histogram of amplitudes (right) for a sample of red variables from OGLE-II data. The location of the vertical line indicates the adopted amplitude threshold for Mira variables.

trum. The histogram of amplitudes for LPVs with  $\log(P)$  larger than 2.0 is bimodal (Mattei et al. 1997) with reasonably good separation between lower amplitude semi-regular variables (SR) and Miras (M).

We begin by calculating the total amplitude  $A$  for all  $2 \times 10^5$  objects in the OGLE-II database of DIA photometry using a running median filter with 11 points and taking the difference between extreme values. A sample dominated by LPVs is obtained by requiring  $A > 0.8$  mag. This selects 842 stars variable on time scales of 2 weeks or longer. Periods are obtained using the Analysis of Variance algorithm (AOV; Schwarzenberg-Czerny 1989). The period-amplitude diagram and the histogram of amplitudes for all 842 stars is shown in Figure 1. The gap separating semi-regulars and Miras is clearly visible at  $A \simeq 1.2$  mag (c.f. Cioni et al. 2001 and Eggen 1975). As an independent cross-check, we examine near-infrared colors of candidate stars from the Two Micron All Sky Survey (2MASS<sup>1</sup>). We require a positive identification with a 2MASS point source object within a 1'' radius of the OGLE position. Almost all identified stars have  $(J - H)$  and  $(H - K_s)$  colors consistent with AGB variables observed through the reddening screen equivalent to  $A_v \simeq 0\text{--}2$  mag of visual extinction. We reject only 3 out of 705 positively identified stars, those having  $(J - H) < 0.75$  and  $(H - K_s) < 0.3$ . After verifying the 2MASS colors we select a sample of Mira variables using amplitude ( $A > 1.2$  mag) and period ( $P > 100$  days).

### 2.3. Quality thresholding

Our analysis is limited to the highest quality data, i.e. light curves with the faintest measurement of  $I < 15.0$ . In this magnitude range the photon noise is not a dominant part of the error budget and the influence of crowding is relatively small. Further, only measurements without processing flags are accepted to avoid possible problems due to saturation, unreliable PSF fits, exceptionally large seeing FWHM etc. Finally, measurements with unusually large error bars are rejected. The median and the standard deviation  $\sigma$  around the median are calculated for all error bars in a given light curve. Points with an error bar more than  $4\sigma$  larger than the median error are removed from the analysis. The latter cut removes only 465 points out of 105,890 and has no influence on our conclusions (Section 3.1). The final sample consists of 105,425  $I$ -band measurements of 485 Mira type variables.

## 3. METHOD

<sup>1</sup> This publication makes use of data products from the Two Micron All Sky Survey, which is a joint project of the University of Massachusetts and the Infrared Processing and Analysis Center/California Institute of Technology, funded by the National Aeronautics and Space Administration and the National Science Foundation.

### 3.1. Signature of microvariability

If microvariability events by tenths of a magnitude or more with durations larger than  $\sim 0.1$  days are present, then they should be visible as a tail of photometric outliers. Some of the outliers could be statistical fluctuations in the measurements, so by assuming that all such outliers are due to rapid variability in the sources we obtain an upper limit on the frequency of such events. One can only afford such a conservative assumption and still derive a useful limit when the data quality is very high and the contribution from random measurement errors to the tail is negligible.

To define the normal behavior of an object with respect to which we measure the outliers, we fit a smooth curve to the data. Using  $\chi^2$  minimization, each season for the light curves is fitted separately with a model consisting of a set of harmonics:

$$m_I(t) = A_0 + \sum_{k=1}^7 (A_k \sin(k\omega t) + B_k \cos(k\omega t)), \quad (1)$$

where  $\omega = 2\pi \text{ yr}^{-1}$ . This model is smooth on time scales of 26 days or longer. The choice of any particular model is not important as long as it is smooth on time scales of about 1 month and still fits the long term behavior of the Mira flux. Oscillating functions can usually achieve that with fewer parameters than other basis functions.

It is important to verify that the model does not over-fit the data, as this would suppress the detection of outliers. In Figure 2 we present a few examples of OGLE-II light curves for Mira stars used in our calculations. There is some limited potential for over-fitting near the beginning and the end of each observing season, especially if one or two points are somewhat separated from the rest of the measurements in a particular season. This is unavoidable as the model for normal behavior of the flux near such loose points is effectively undefined. But within the observing season there is very little possibility that a model smooth on time-scales of 1 month (Figure 2) can fit individual points. The temporal spacing of measurements is too fine for that in most cases. Nevertheless, in order to make any conclusions about the rate of microvariability, the influence of this and other possible effects has to be fully quantified with the proper efficiency calculation. We present such a calculation in Section 3.3.

The approach taken by dL98 in the Hipparcos analysis is not possible for OGLE-II data. Hipparcos light curves consist of brief observing sequences lasting typically less than 1 day but densely sampled with measurements often separated by about 20 minutes. This is why long term variations of the main Mira cycle are not an issue and at the same time many events can be resolved. The time sampling of the OGLE-II light curves is generally not sufficient to resolve any rapid variability on time-scales shorter than 1 day. Typically the density of measurements well within the observing season corresponds to one point every 1 to 3 days and it tapers off near both ends of the season. Some variations of temporal sampling arise due to changing observing conditions. Still, there are 1046 pairs and 210 triples of observations spanning less than 24 hours. Those better sampled regions significantly improve the sensitivity to the shortest events

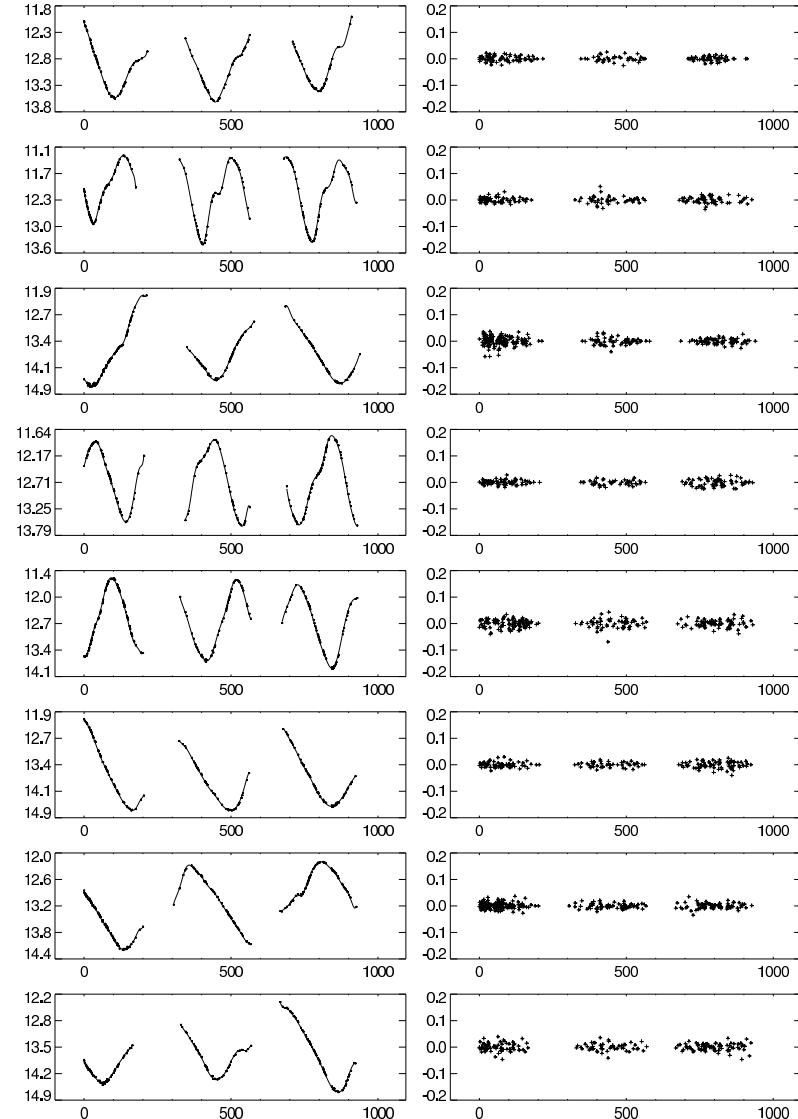


FIG. 2.— Examples of OGLE-II light curves for Mira variables in the Galactic Bulge with model fits given by Equation 1 (left). Also shown are photometric residuals with respect to the model (right). All units are  $I$  magnitude versus time in days. Note that the amplitudes of all events reported by dL98 exceed the largest residuals by a factor of  $\sim 5$ .

considered in our analysis. At the basis of our approach is exceptionally good error distribution in the OGLE-II DIA photometry combined with the ability to fit longer term behavior of the Mira flux. Even if microvariability events are infrequent and very short, each object with rapid variations discovered by dL98 spends some (small) fraction of time in the events, when the object flux is far from the normal smooth trend of the main pulsation cycle. Eventually, with persistent monitoring, some measurements will be affected by microvariability regardless of the time sampling.

We define an “event” as one or more consecutive measurements deviating (consistently) up or down by more than 0.2 mag with respect to the best fit model of Equation 1. Experiments requiring two consecutive deviations (a two-point filter) and 0.15 mag limit for the flux departure generally confirm our conclusions, albeit at a factor

of 2 to 10 lower sensitivity. In both searches we detect no events.

We checked the impact of the last selection cut from Section 2.3 which removes points with unusually large error bars. Without this condition imposed, only three single point “events” in the entire data set depart from the model by: 0.21, -0.25, 0.23 mag. Two of them originate from the same frame, and all have error bars much larger than the rest of the corresponding light curve, particularly the neighboring points. They are much more likely manifestations of a problem with the measurement rather than detections of microvariability. It is safe to conclude that we have not detected any rapid variability events.

### 3.2. Probability density for event rate

Counting events from Section 3.1 is a Poisson process with the expectation value  $\mu = \sum_s \nu T \epsilon_s = \nu \mathcal{E}$ , where  $\nu$

is the yearly rate of actual physical events per object of the ensemble,  $T$  is the duration of the survey and  $\epsilon_s$  is the efficiency of detecting an event that occurred randomly during the survey time in star  $s$ . We substitute  $\mathcal{E} = T \sum_s \epsilon_s$  to simplify notation. In other words  $\mu$  is the total expected number of events in the entire sample of 485 stars observed for  $T = 3$  years assuming that every star undergoes  $\nu$  events per year on average. Equivalently, if only a fraction of the stars experienced events, the rate  $\nu$  would be proportionately higher in those objects. Using Bayes' theorem we can derive the probability distribution for the rate given the number of observed events  $n$ :

$$P(\nu|n) = \frac{P(n|\nu)P(\nu)}{P(n)}, \quad (2)$$

where  $P(n|\nu) = \mu^n \exp(-\mu)/n!$  is the Poisson distribution and  $P(n)$  is the normalization factor obtained from condition  $\int_0^\infty P(n|\nu)d\nu = 1$ . For lack of other knowledge we also assume a uniform prior probability for the rate  $P(\nu) \equiv 1$ . This results in the following probability distribution for  $\nu$ :

$$P(\nu|n) = \frac{\mathcal{E}^{n+1}}{n!} \nu^n \exp(-\nu\mathcal{E}). \quad (3)$$

In the case of a non-detection  $P(\nu|n=0) = \mathcal{E} \exp(-\nu\mathcal{E})$  which can be integrated for a confidence level  $\alpha$  to obtain the upper limit for the rate:

$$R_\alpha = \frac{-\ln(1-\alpha)}{\mathcal{E}}. \quad (4)$$

In the following discussions we will use  $R_{95}$ , the 95% confidence upper limit for the event rate.

### 3.3. Simulating efficiency

The term  $\mathcal{E}$  is the crucial piece of information and can be evaluated with the use of a Monte Carlo simulation. We consider microvariability events with two kinds of flux profiles: triangular and instantaneous rise with exponential decay (Sections 4.1 and 4.2 respectively). The time-scale ( $\tau$ ) and the amplitude of a simulated event ( $\Delta m$ ) are drawn from their assumed distributions. A random epoch within the three-year survey baseline is also generated and the flux variation is injected at that epoch. Finally, we attempt to detect the event using the same procedure employed with the real observations in Section 3.1. This includes re-fitting the empirical curve describing normal smooth behavior. For each of the 485 stars in the ensemble, we generate 1000 trial events and count all successful detections.

## 4. RESULTS

### 4.1. Derived rate of Hipparcos events

The distributions of time-scales and amplitudes for microvariability events reported by dL98 are shown in Figure 3. For the purpose of constraining the rates of these types of event, the simulated event time-scales and amplitudes are drawn from the actual observed distributions. There were approximately as many upward and downward deviations reported in the Hipparcos data. We verified that the two distributions appear uncorrelated. In all our simulations we assume that the event amplitude

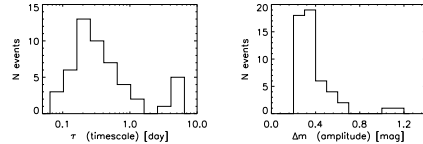


FIG. 3.— Distribution of time scales (left) and amplitudes (right) of events reported by de Laverny et al. (1998).

is independent of the time-scale and the sign of the deviation is random. The shape of the artificial impulse is a triangle with the base covering the time interval  $\pm\tau$ . In Section 4.2 we will see that the results are not very sensitive to that choice.

Figure 4 shows the probability distributions for the event rate  $\nu$  given  $n = 0, 1, 2$ , and 3 detections. Given that we have detected  $n = 0$  events in the OGLE-II data, the upper limit for the rate (95% confidence) is  $R_{95} = 0.038 \text{ yr}^{-1}$  per star. We conclude, with 95% probability, that dL98 type events are less frequent than 1 every 26 years in any given object of our OGLE  $I$ -band sample.

The study of dL98 does not give the value for the efficiency of the Hipparcos light curves in detecting Mira microvariability. In order to derive the event rate implied by results of dL98 we need to know the detection efficiency. We can estimate it using public Hipparcos data from the Epoch Photometry Annex (ESA 1997). For any given object the Hipparcos observing sequences cover only a small fraction of the total duration of the experiment. Observing sequences are typically separated by gaps lasting about two weeks. Any events occurring in those gaps cannot be detected; the instrument is simply not observing the object. We extracted light curves for 226 Hipparcos stars classified as Miras in GCVS. This is fewer than 239 light curves analyzed by dL98, but includes objects contributing 50 out of 51 reported events<sup>2</sup>. We adopt 3.37 years as the total duration of the Hipparcos mission, taking the difference between the first and the last epoch in all 226 light curves. For each light curve we subtract from the total duration the sum of all gaps lasting 10 days or longer and divide the result by the total duration. On average there were 104 photometric points available per star. We do not remove any flagged points. This and the implicit assumption of 100% efficiency within observing sequences will only increase the final value of the efficiency and lower the rate.

The distribution of the resulting efficiencies for Hipparcos data is shown in Figure 5 and compared to the results of our Monte Carlo experiments with OGLE-II data. For a few Hipparcos stars events can be detected with relatively high efficiency reaching 20–40%. However, for the majority of the Hipparcos light curves the efficiency is similar to that for OGLE-II data. The additional Monte Carlo run on OGLE-II data with the distribution of time-scales from dL98 truncated at  $\tau > 2$  days demonstrates that our results do not depend dramatically on the presence of the long duration tail.

If  $\nu$  is the true yearly rate of events in units of  $\text{yr}^{-1}$

<sup>2</sup> There seems to be a problem with identification of the 51st event in variable CE Lyr. The on-line Hipparcos catalog entry for the star closest to the GCVS position states that the star may be wrongly identified with CE Lyr. The star appears constant. In any case, these minor differences are unimportant.

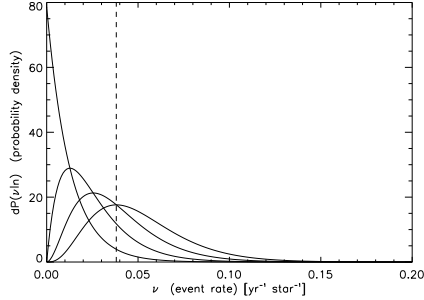


FIG. 4.— Probability distributions for the rate of events of the de Laverny et al. (1998) type. Lines correspond to probabilities given that there were between  $n = 0$  (farthest left) to  $n = 3$  (farthest right) detections. The location of the vertical line indicates the 95% confidence upper limit for the rate given a non-detection.

$\text{star}^{-1}$ , the expected number of events over the total duration of the experiment (detected or not) is:  $\nu NT$ , where  $N$  is the total number of monitored objects and  $T$  is the duration of the experiment in years. On the other hand, the total number of events can be recovered from the number of detected events by counting each detection with the weight proportional to the inverse of the efficiency:  $\sum_s n_s/\epsilon_s$ , where  $n_s$  is the number of detected events in star  $s$  and  $\epsilon_s$  is the efficiency of detecting a random event in star  $s$ . The number of detections per star in dL98 study is between 0 and 3. By equating the two above expressions one obtains an estimator of the event rate:

$$\nu = \frac{1}{NT} \sum_s \frac{n_s}{\epsilon_s} \quad (5)$$

We evaluate the rate in Equation 5 using our efficiency estimates for a sample of  $N = 226$  Hipparcos light curves and accepting all detections reported by dL98 (except the one in CE Lyr for which we could not find the data). As mentioned earlier, the efficiency was likely over-estimated so the rate is likely under-estimated. The resulting rate is  $1.63 \text{ yr}^{-1} \text{ star}^{-1}$ . Therefore, the Hipparcos results imply that microvariability events in Miras are quite common in the spectral region covered by the  $H_P$  band. This is due to the fact that, assuming the events are not correlated with the scheduling of the Hipparcos observing sequences, for every detected event there were  $\sim 25$  events that could not be detected due to a gap in coverage. The effective efficiency is only  $\sim 4\%$  and comparable to that of the OGLE-II observations. Taken at face value, the OGLE-II data appear inconsistent with high rates implied by the number of Hipparcos detections. Given a true rate of 1 event per year per object, the probability that an ensemble like ours would yield 0 detections is less than  $6 \times 10^{-35}$ . However, there are several scenarios that can easily accommodate both our non-detection in the  $I$  filter and the positive Hipparcos result in the  $H_P$  band. We discuss this issue further in Section 5.

#### 4.2. Constraining flashes on Miras

Several possible mechanisms for rapid light variations in Mira variables have been discussed by Willson and

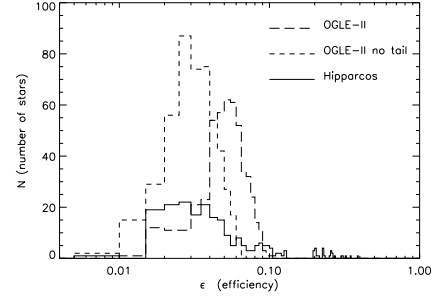


FIG. 5.— Results of the Monte Carlo efficiency experiments with OGLE-II data compared to a conservative estimate of the efficiency for Hipparcos data. The thin short-dash line is for the Monte Carlo run on OGLE-II data using the distribution of time-scales from dL98 truncated above  $\tau = 2$  days.

Struck (2002). One such scenario invokes a sudden release of energy leading to "hot flashes". We can put useful constraints on such events by simply simulating the efficiency of detecting a different kind of flux impulse in our data. This also provides a cross-check on the results from Section 4.1, and in particular shows how sensitive the derived limits on frequency are with respect to the pulse shape. In this section we adopt a flare with instantaneous rise by  $\Delta m$  and exponential decay time  $\tau$ . The average efficiency (per star) of detecting such flares is shown in Figure 6. The dependence on the flare amplitude between 0.3 and 1.1 mag is plotted for a number of time scales  $\tau$  ranging from 0.1 to 1.6 days. Note that the figure shows that flashes with amplitudes of a few tenths of a magnitude lasting only a couple hours can be detected with the efficiency of a few percent in any of the stars in our ensemble.

Before deriving the upper limits on rates, we introduce the size-frequency distribution into this calculation. The published data offers very little information on the properties of suspected flares, but one generally expects strong events to occur less frequently and weak events to dominate. For the purpose of illustrating the range of possible outcomes, we assume a power-law distribution of  $f = \Delta F/F$  the amplitude of the simulated flashes relative to the flux  $F$  of the parent star:

$$N(f)df \propto f^{-\gamma} df \quad (6)$$

At fixed time scale  $\tau$  and parent star flux  $F$  this size distribution is equivalent to assuming a power-law distribution of flare energies. The distribution is truncated below the relative flare amplitude of 20% and above 100%, which corresponds to amplitudes of about 0.2 and 0.75 mag respectively.

Taking the amplitude distribution of dL98 and ignoring the sign of the variation,  $\gamma$  between 2.0 and 2.5 gives a good approximation within the limited statistics of the data set. We evaluate the efficiency at several fixed time scales ranging from 0.1 to 2.0 days for a power-law size frequency distribution with index  $\gamma = 1, 2$  and 3. The resulting rates are given in Figure 7. The frequency of 1 per 2.5 years in any given star is excluded with 95% probability for all types of considered events down to durations of 2.4 hours. The limits quickly tighten for longer flare durations. For  $\gamma = 2$  we can exclude 0.5 day long events being more frequent than about once every

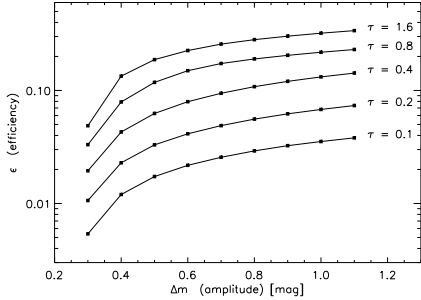


FIG. 6.— Simulated efficiency of detecting flashes with instantaneous rise and exponential decay. The dependence on amplitude  $\Delta m$  is given for several fixed time scales  $\tau$ .

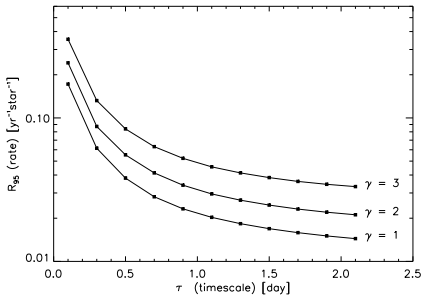


FIG. 7.— Upper limits (95% confidence) on the rate of flashes on Mira variables given a non-detection in our ensemble. The dependence on time scale is given for three power law distributions of fractional flux amplitudes with the index  $\gamma = 1, 2$ , and  $3$  (Section 4.2).

17 years.

## 5. DISCUSSION

Using a large sample of objects with high quality light curves we place stringent limits on the frequency of rapid variability events in the Galactic Bulge Mira variables in the  $I$  band. To the best of our knowledge this is the first published limit for the rate of rapid variability in Miras. The study is most sensitive to events lasting about 1 day or longer, however it retains a few percent efficiency (per star) for detecting unresolved microvariability on time scales as short as 2 hours. With 95% probability we excluded events of the type found by dL98 occurring more frequently than 1 per 26 years in the average object of our sample ( $0.038 \text{ yr}^{-1} \text{ star}^{-1}$ ). The results are not sensitive to the details of the temporal profile of the flares. The most significant dependence of the detection efficiency in our ensemble is on the event time scale because of the 1–3 day light curve sampling. The limits on the frequency of flashes with a sudden flux rise and exponential fall-off with power-law distribution of energies (at fixed parent star luminosity) have been presented. For flare durations ranging from 0.1 to 1 day the corresponding limiting rates are between once every few years and once every few tens of years.

In our calculations we essentially extrapolate the properties of the rapid variability events observed by Hipparcos from  $H_P$  band to the  $I$  band. Under that assumption, the OGLE-II data are inconsistent with high rates implied by the number of Hipparcos detections. A possible explanation is that the microvariability is much less prominent or the events are shorter in the  $I$  band. In that case we are still learning something about microvariabil-

ity in Mira stars. The typical accuracy of the OGLE-II photometry is much better than 0.2 mag (Figure 2) and we could not find any indication of rapid variations in any of the 485 studied objects. All light curves have very smooth appearance.

There are at least three possible explanations for the difference between the two results:

1. Mira variables in the Galactic Bulge population differ from their counterparts in the solar neighborhood. In the scenario of a planet interacting with the Mira atmosphere, e.g., the Bulge population might not have any planets. It is plausible that the Galactic Bulge Miras have lower metallicity than a typical Hipparcos star. Planets are more prevalent around metal-rich stars (e.g. Santos, Israelian, & Mayor 2004). It has been suggested that dust may play an important role in microvariability of Miras (Stencel et al. 2003). The dust content of the stellar envelope could be related to metallicity.
2. Microvariability in Miras is occurring in the part of the spectrum that is not covered by Cousins  $I$  band but is contributing to the blue part of the  $H_P$  band.
3. Microvariability in Miras is less common than implied by results of dL98. The only sure way to verify this is to collect more data and carefully analyze it. Numerous groups are setting up fast cadence photometric monitoring experiments with the goal of detecting real time transients (Vestrand et al. 2002) or finding transiting Jovian planets (Horne 2003). Teets & Henson (2003) are conducting a special purpose monitoring campaign of  $\sim 5$  sources previously reported to display rapid variability using  $B, V, R, I$  filters. The current data set covers many nights spanning the time interval of over 2 years with up to 5 photometric points per hour for up to 8 hours a night. So far only a single event in RR Boo has been detected. With the available phase coverage this is far below expectations based on the Hipparcos data.

The  $H_P$  filter of the Hipparcos mission is broader than  $V$  and still sensitive in the wavelength range 650–900 nm, where the spectral energy distribution of a Mira variable rises steeply. We can calculate the amount of energy emitted by a Mira star in the  $H_P$  band knowing that the ratio of luminosities in  $H_P$  and  $V$  is about 2.5. This is easily estimated assuming that the spectrum of a Mira star blue-ward of 1000 nm is a black body with effective temperature  $T_{eff} = 2500$  K and by folding it with filter transmission curves (Johnson 1965, van Leeuwen et al. 1997). Then using the absolute magnitudes  $M_V = -0.3$  of an M5 giant and the  $V$ -band Solar luminosity  $L_{V,\odot} = 4.64 \times 10^{32} \text{ erg s}^{-1}$  (Binney & Merrifield 1998) we obtain  $L_{H_P} = 1.3 \times 10^{35} \text{ erg s}^{-1}$  for a Mira star. We adopt  $M_{V,\odot} = 4.83$ . Mira variables vary considerably less in the  $H_P$  band compared to  $V$  with amplitudes rarely exceeding 4 mag (Whitelock, Marang & Feast 2000). Even during minimum light and taking an extreme value for the amplitude (4 mag) the total energy of a flare with amplitude  $\Delta m$  and duration  $\tau$  is:

$$E = 2.8 \times 10^{38} \text{ erg} \times C \times \left( \frac{\tau}{1 \text{ day}} \right) \times \left( 10^{0.4|\Delta m|} - 1 \right), \quad (7)$$

where  $C$  is the numerical factor depending on the profile of the light variation. For a top hat function  $C = 1$ . We can see that a flare of a third of a magnitude lasting 24 hours will require  $10^{38}$  ergs of energy—an order of magnitude more than the energy required for the same contrast in the  $V$  band calculated by Willson & Struck (2002). If in fact the events detected by Hipparcos are confirmed, one will be faced with finding a large energy source that is triggered approximately as often as an energy sink of

the same size. The observational evidence is accumulating and it should not be long before we can formulate a more definitive answer to the exciting question of rapid high amplitude variability on Miras.

## REFERENCES

Binney, J., & Merrifield, M. 1998, Galactic Astronomy (Princeton, NJ: Princeton University Press)

Cioni, M. R. L., Marquette, J. B., Loup, C., Azzopardi, M., Habbing, H. J., Lasserre, T., & Lesquoy, E. 2001, *A&A*, 377, 945

de Laverny, P., Geoffray, H., Jorda, L., & Kopp, M. 1997, *A&AS*, 122, 415

de Laverny, P., Mennessier, M. O., Mignard, F., & Mattei, J. A. 1998, *A&A*, 330, 169 (dL98)

Eggen, O. J. 1975, *AJ*, 195, 661

ESA 1997, The Hipparcos and Tycho Catalogues, ESA SP-1200

Horne, K. 2003, preprint (astro-ph/0301249)

Johnson, H. L. 1965, *ApJ*, 141, 923

Keeley, D. A. 1970, *ApJ*, 161, 657

Kholopov, P. N. 1998, General Catalog of Variable Stars (4th ed.; Moscow: Nauka)

Kovar, R. P., Potter, A. E., Kovar, N. S., & Trafton, L. 1972, *PASP*, 84, 46

Mattei, J. A., Foster, G., Hurwitz, L. A., Malatesta, K. H., Willson, L. A., & Mennessier, M. O. 1997, in Proc. of the ESA Symposium 402, Hipparcos-Venice '97, ed. B. Battrick, M. A. C. Perryman, & P. L. Bernacca (ESA Publication Division: Noordwijk, The Netherlands), 269

Odell, A., Vrba, F., Fix, J., & Neff, J. 1970, *PASP*, 82, 883

Santos, N. C., Israelian, G., & Mayor, M. 2004, *A&A*, 415, 1153

Schaefer, B. E., King, J. R., & Deliyannis, C. P. 2000, *ApJ*, 529, 1026

Schwarzenberg-Czerny, A. 1989, *MNRAS*, 241, 153

Smak, J., & Wing, R. F. 1979, *Acta Astron.*, 29, 199

Smith, B. J., Leisawitz, D., Castelaz, M. W., & Luttermoser, D. 2002, *AJ*, 123, 948

Stencel, R. E., Ostrowski-Fukuda, T. A., Jurgenson, C. A., & Phillips, A. 2003, in *ASP Conf. Series, Proceedings of the 12th Cambridge Workshop on Cool Stars, Stellar Systems and the Sun*, eds. A. Brown, G. M. Harper, & T. R. Ayres, (San Francisco: ASP), in press

Struck, C., Cohenim, B. E., & Willson, L. A. 2002, *ApJ*, 572, L83

Struck, C., Cohenim, B. E., & Willson, L. A. 2004, *MNRAS*, 347, 173

Teets, W. K., & Henson, G. D. 2003, *BAAS*, 35, 1217

Udalski, A., Kubiak, M., & Szymański, M. 1997, *Acta Astron.*, 47, 319

Vestrand, W. T., et al. 2002, in *Proc. of SPIE, 4845, Advanced Global Communications Technologies for Astronomy II*, ed. by R. I. Kibrick, (Bellingham: SPIE), 126

Whitelock, P., Marang, F., & Feast, M. 2000, *MNRAS*, 319, 728

Willson, L. A., & Struck, C. 2002, *J. AAVSO*, 30, 23

Woźniak, P. R. 2000, *Acta Astron.*, 50, 421

Woźniak, P. R., Udalski, A., Szymański, M., Kubiak, M., Pietrzyński, G., Soszyński, I., & Źebrun, K. 2002, *Acta Astron.*, 52, 129

van Leeuwen, F., Evans, D. W., Grenon, M., Grossmann, V., Mignard, F., & Perryman, M. A. C. 1997, *A&A*, 323, 61